ELSEVIER

Composites: Part B 33 (2002) 263–277

composites
Part B: engineering

www.elsevier.com/locate/compositesb

The revolutionary creation of new advanced materials—carbon nanotube composites

Kin-Tak Lau[a,*], David Hui[b]

[a]Department of Mechanical Engineering, The Hong Kong Polytechnic University, Hung Hom, Kowloon, Hong Kong, People's Republic of China
[b]Department of Mechanical Engineering, University of New Orleans, New Orleans, LA, USA

Received 14 January 2002; accepted 25 February 2002

Abstract

Since the discovery of carbon nanotubes at the beginning of the last decade, extensive research related to the nanotubes in the fields of chemistry, physics, materials science and engineering, and electrical and electronic engineering has been found increasingly. The nanotubes, having an extreme small physical size (diameter $\approx$ 1 nm) and many unique mechanical and electrical properties depending on its hexagonal lattice arrangement and chiral vector have been appreciated as ideal fibres for nanocomposite structures. It has been reported that the nanotubes own remarkable mechanical properties with theoretical Young's modulus and tensile strength as high as 1 TPa and 200 GPa, respectively. Since the nanotubes are highly chemical insert and able to sustain a high strain (10–30%) without breakage, it can be foreseen that nanotube-related structures could be designed for nanoinstrument to create ultra-small electronic circuits and used as strong, light and high toughness fibres for nanocomposite structures. In this paper, recent researches and applications on carbon nanotubes and nanotube composites are reviewed. The interfacial bonding properties, mechanical performance and reliability of nanotube/polymer composites will be discussed.

Keywords: A. Fibres; B. Fracture; A. Nanostructures; B. Mechanical properties; Carbon nanotubes

1. Introduction

The formation of carbon nanotubes could be traced back to the discovery of the fullerence structure C_{60} (buckyball) in 1985 [1]. The structure of the buckyball comprises of 60 carbon atoms arranged by 20 hexagonal and 12 pentagonal faces to form a sphere, when the buckyball is elongated to form a long and narrow tube with a diameter of approximately 1 nm (10 Å), which is the basic form of a carbon nanotube (it will be simply called a 'nanotube' in the rest of this paper). In 1991, a Japanese electron microscopist Iijima [2] has discovered fullerence-related structures, which consist of multi-graphene cylinders closed at either end with caps containing pentagonal rings by a direct-current arc discharge between carbon electrodes immersed in helium gas under a temperature of 3000 °C, the multi-walled nanotubes (MWNTs) were created. Structurally, the shape of a single-walled nanotube (SWNT) could be imagined that a graphene sheet rolls into a tubule form with end seamless caps together with very high aspect ratios of 1000 or more [3]. As individual molecules, the SWNT is believed to be a mostly defect-free structure leading a high strength despite their low density [4]. In Fig. 1(a), the crystal structures of different carbon-based materials are shown. The nanotubes could be formed as a rope consisting of 10–100 nanotubes per bundle in random tangles. In Fig. 1(b), the electronic micrographs of nanotubes with five (left), two (middle) and seven (right) graphene layers are shown. The maximum outer diameter of the nanotubes shown in the figure is about 6.7 nm. In particular application, the space exploration activities requires the structural with a highly weight concern for launch vehicles and space systems, this accelerates the development of materials by incorporating nanotubes into polymeric or other materials to form novel structural members [5].

Nanotubes have extraordinary mechanical, electrical and thermal properties with providing strong, light and high toughness characteristics. It has been estimated that the nanotubes could be designed as a longest cable in the world, i.e. a 23 000 mile cable from space station to the Earth without suffering a high gravitation force due to its own weight at that length [6]. Only the tiny fullerence strands could sustain their weight when spanning 23 000 miles. The tensile modulus and strength of the nanotubes ranging about 270 GPa to 1 TPa and 11–200 GPa,

* Corresponding author.
E-mail address: mmktlau@polyu.edu.hk (A.K.-T. Lau).

1359-8368/02/$ - see front matter
PII: S1359-8368(02)00012-4

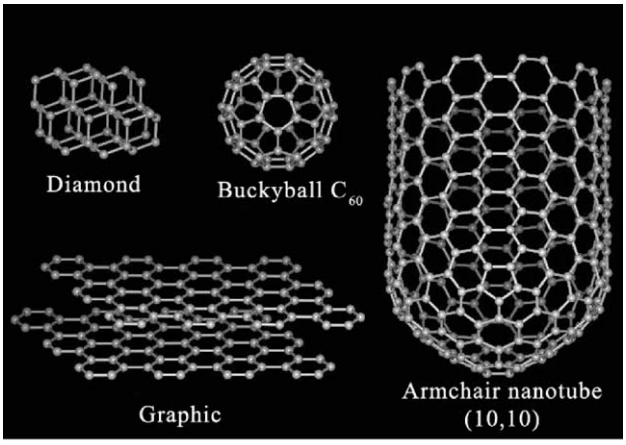

(a)

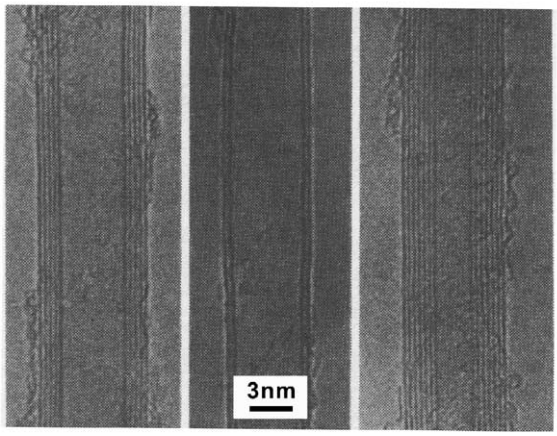

(b)

Fig. 1. (a) Different forms of carbon-based materials (Photo courtesy of Rice University) and (b) electron micrographs of nanotubes with different numbers of graphene layers. The out diameters of the nanotubes are 6.7 nm (left), 5.5 nm (middle) and 6.5 nm (right) [2].

respectively, have been reported recently [7,8]. In Fig. 2, the comparison of the tensile strength of different engineering materials is shown. The nanotubes exhibit an extraordinary performance compared with graphite and Kevlar fibres, and stainless steel. The nanotubes are at least 100 times stronger than steel, but only one-sixth as heavy making it to bolster about any engineering materials. Moreover, the nanotubes own high thermal and electrical conductivities far better than copper enabling it to reinforce tiny structures with bearing a dual function of reinforcement and signal transmitting of composite circuit boards.

In this paper, recent development on the nanotubes and researches in the applications on nanotube composites are reviewed. The fundamental physics of the nanotubes and their electronic and structural properties with different chiralities will be introduced. The major focuses on recent researches have paid much attention on the examination

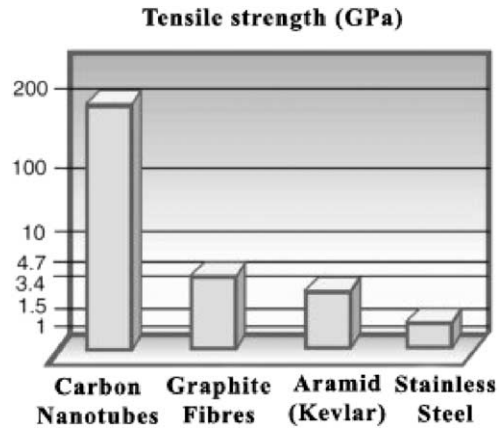

Fig. 2. Comparison of the tensile strength of different engineering materials, in log scale.

of the mechanical properties such as tensile strength of an individual nanotube or a bundle of nanotube-rope, the buckling properties due to shrinkage of matrices after curing and the bending stiffness of nanotube-composite structures. The investigation on the interfacial bonding strength of nanotubes to different matrix environments will also be discussed in this paper.

2. Production of nanotubes

Recently, researches related to the nanotubes have been found in many scientific and engineering literatures, the fields of interest included physics, chemistry, materials science and engineering, and electrical and electronic engineering. The production of the nanotubes with a high order of impurity and uniformity is a one of the big issues that still impacting the nanotubes society. The manufacturing processes of the nanotubes include direct-current arc discharge [9–11], laser ablation [12], thermal and plasma enhanced chemical vapour-growth depositions (CVD) [13,14] and recent developed self-assembly of single crystals of SWNTs [15] methods. Direct-arc discharge and laser ablation methods require the addition of a small amount of metal catalyst, which increases the yield of the nanotubes. The products are normally tangled and in poorly ordered mat although individual tube could be made as several hundred microns long. The differences of lattice arrangement in zigzag, armchair and chiral forms coexist in the products. In addition, these methods require very high temperature (arc charge: 5000–20 000 °C, laser vaporisation: 4000–5000 °C [16]), which make difficult in the control of chirality and diameter of the nanotubes. Nonetheless, the laser ablation has been recognised as tool for mass production of SWNTs [17]. An improved laser ablation method has been developed by using a cobalt coat silica plate to align the growth of nanotubes [18]. The method offers control of overall length ($\approx$50 μm) of the nanotubes and fairly uniform diameters (30–50 nm).

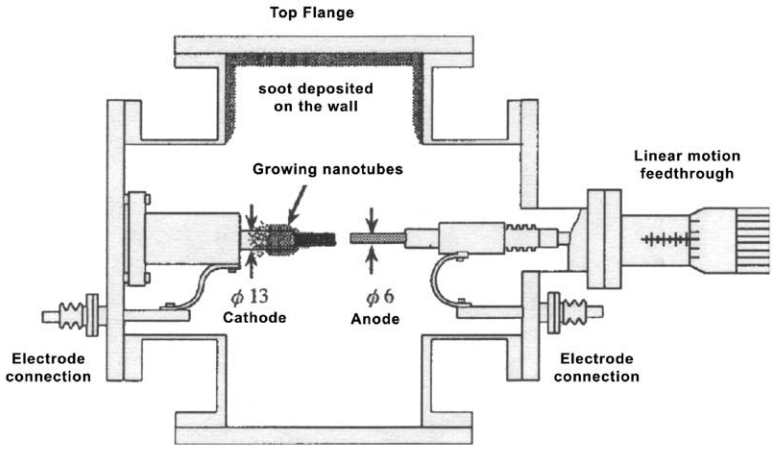

(a)

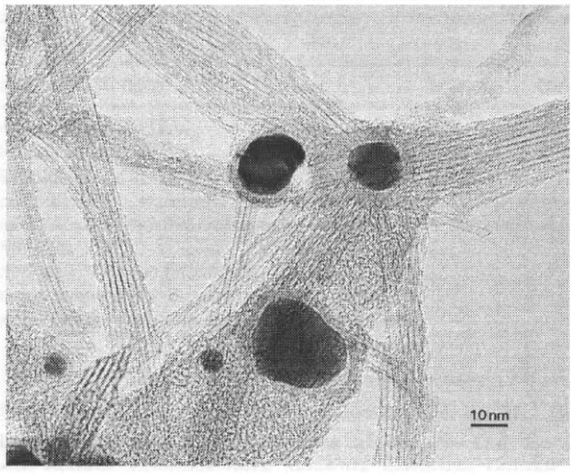

(b)

Fig. 3. (a) Schematic drawing of the direct-current arc discharge method for producing carbon nanotubes and (b) TEM micrograph of single layer nanotube growing from platinum group particles [22].

The CVD has been appreciated as the best method to produce high-purity MWNTs with varying diameters and structures [19]. However, ordered arrays beyond short sections of ordered nanotubes have not yet produced and the chirality and diameter of the nanotubes cannot be controlled precisely. In Figs. 3–5, the schematic diagrams of different methods of the production of nanotubes and the scanning electronic microscopy (SEM) images of the nanotubes are shown. In the figures, it is obviously seen that the nanotubes made by direct-current arc discharge and laser ablation methods produced a bundle of SWNTs, which are curved and entangled while the nanotubes made by the self-oriented regular arrays [20] and plasma enhanced chemical vapour depositions [21] exhibit more straight and uniform growth.

Recently, Schlittler et al. [15] have developed a better method that allows making nanotubes in an ordered array of nanotubes with identical diameter, chirality and straight with a high purity. In Fig. 6, a schematic deposition process of C_{60} and Ni to produce nanotubes growing on a molybdenum substrate is shown. The mixture of C_{60} and Ni is evaporated through a nanostencil mask with an array of 300 nm diameter holes, which is accurately positioned a few microns above a surface and able to move with sub-nanometer precision during the evaporation process. The selection of the substrate materials is crucial since the substrate should be able to constrain the C_{60} and Ni at an original 300 nm diameter evaporation area during diffusion process at high temperature. Latest studies found that the use of molybdenum substrate could provide an excellent results either in the form of a grid for transmission electron microscope (TEM) investigation or as a solid film sputtered

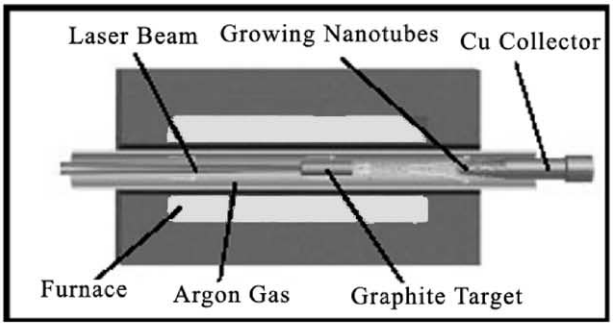

(a)

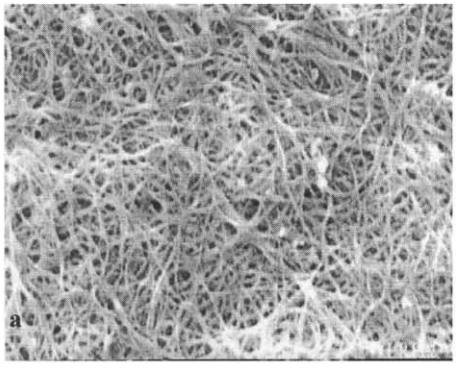

(b)

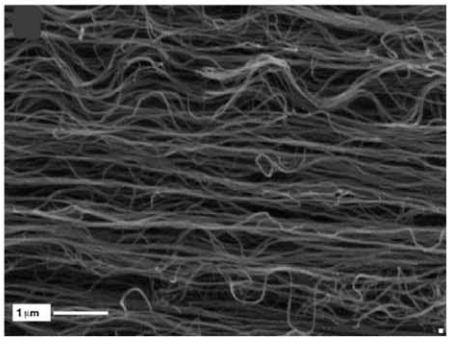

(c)

Fig. 4. (a) Schematic drawing of the laser ablation process [23]. (b) SEM images of the collected nanotubes after the first stage filtration [12]. (c) Aligned nanotube bundle by using a cobalt coat silica plate to align the growth of nanotubes [18].

onto a silicon wafer [15]. The presence of the magnetic field controls the growth direction of the nanotubes. Fig. 7 depicts the view of SWNTs grown on a molybdenum substrate by using the SEM.

3. Physics of carbon nanotubes

3.1. Structure of nanotubes

In the early 1960, Feynman [24] has predicted that the

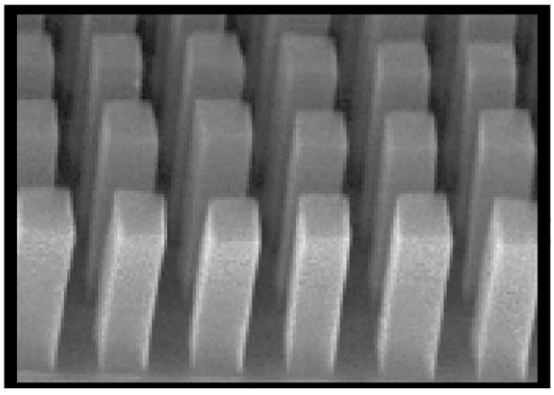

(a)

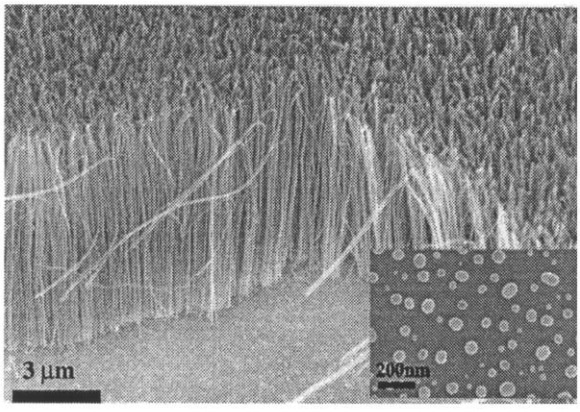

(b)

Fig. 5. (a) SEM images of nanotube towers synthesised on 38 μm by 38 μm catalyst patterns [20] and (b) the well grown of nanotubes by using plasma-induced alignment method [21].

future science and technology would be focused on miniaturisation, in which the electric motors would be designed as small as the size of the nail on your small finger. Every machine, structure and instrument would be designed starting from atomic scale. At that time, only physicists and chemists would interest in dealing with the works in such small scale. Until 1991, the discovery of nanotubes has revolutionised researches in many different directions. A light and high strength nanotubes would be an ideal structural member for designing nanostructural instrument and nanocomposite structures. Port [25] has reported that nanotubes and nanocomposites could become as familiar as silicon in this century and the full development of the nanotubes would be around 2010. In order to familiarise the uses and applications of the nanotubes and its related products, an understanding of the structure, characterisations and properties of the nanotubes is essential.

Nanotubes are fullerene-related structures, which like to roll a piece of graphene sheet to form a cylinder with end

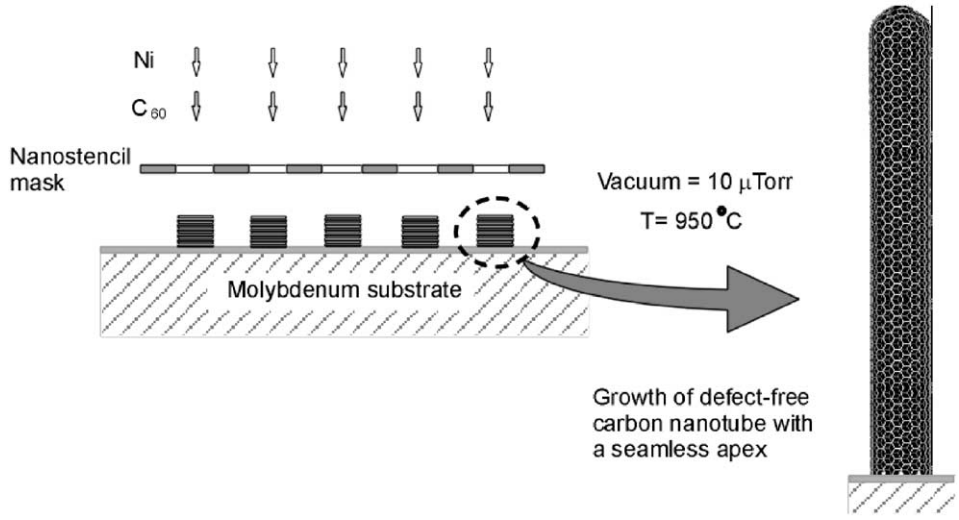

Fig. 6. A schematic deposition process by which C_{60} and Ni are alternatively evaporated through a 300 nm diameter nanostencil mask to produce nanotubes under a controlled temperature and pressure.

caps containing pentagonal rings. It has been found during the arc-evaporation synthesis of fullerenes process as mentioned previously. The closed graphical structures including nanoparticles and nanotubes were formed at the central core of the cathodic deposit (Fig. 3(a)). The nanotubes possess conducting properties ranging from metallic to moderate band gap semi-conductor [26]. In general, the nanotubes could be specified in terms of the tube diameter d, and the chiral angle θ, which are shown in Fig. 8. The chiral vector C_h is defined as a line connected from two crystallographically equivalent sites O and C on a two-dimensional graphene structure. The chiral vector can be defined in terms of the lattice translation indices (n, m) and the basic vectors a_1 and a_2 of the hexagonal lattice (a layer of graphene sheet) [27], i.e.

$$C_h = na_1 + ma_2 \quad (1)$$

The chiral angle, θ, is measured an angle between the chiral vector C_h with respect to the zigzag direction $(n, 0)$, where $\theta = 0$ and the unit vectors of a_1 and a_2. The armchair nanotube is defined as the $\theta = 30°$ and the translation indices is (n, n). All other types of nanotubes could be defined as a pair of indices (n, m), where $n \neq m$. The electronic conductivity is highly sensitive to a slight change of these parameters, which cause a changing of materials between metallic and semi-conducting statuses. Recently, it has been reported that the scanning tunnelling microscopy (STM) and spectroscopy could be used to observe the electronic properties and atomic arrangement of SWNTs [28]. In Fig. 9(a), the models of different types of SWNTs are shown, which gives a more clear understanding of the structure of the nanotubes [1]. Fig. 9(b) gives an image of a zigzag (15, 0) SWNT [29]. In Table 1, parameters, which are used to determine the geometry of the SWNT are listed [30]. According to the

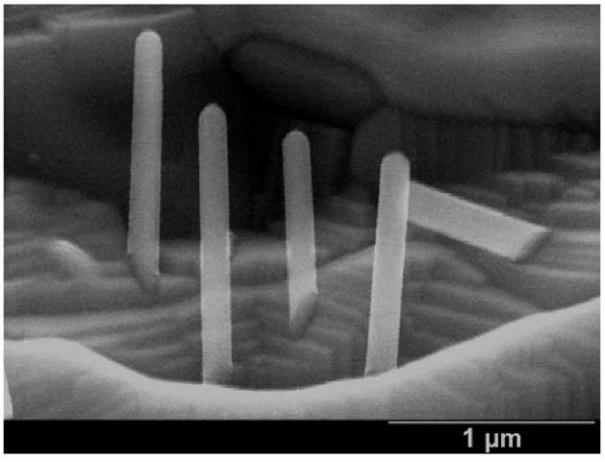

Fig. 7. The grown of carbon nanotubes on the molybdenum substrate [15].

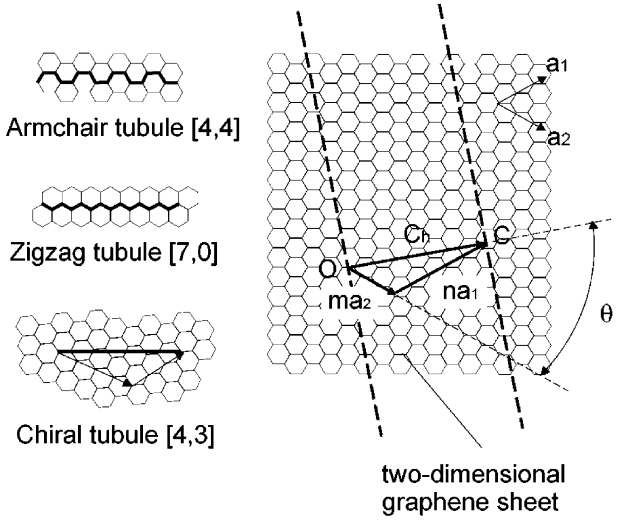

Fig. 8. The chiral vector OC or $C_h = na_1 + ma_2$ is defined on the hexagonal lattice of carbon atoms (a graphene sheet) by unit vectors a_1 and a_2 and the chiral angle θ with respect to the zigzag axis, i.e. $(n, 0)$.

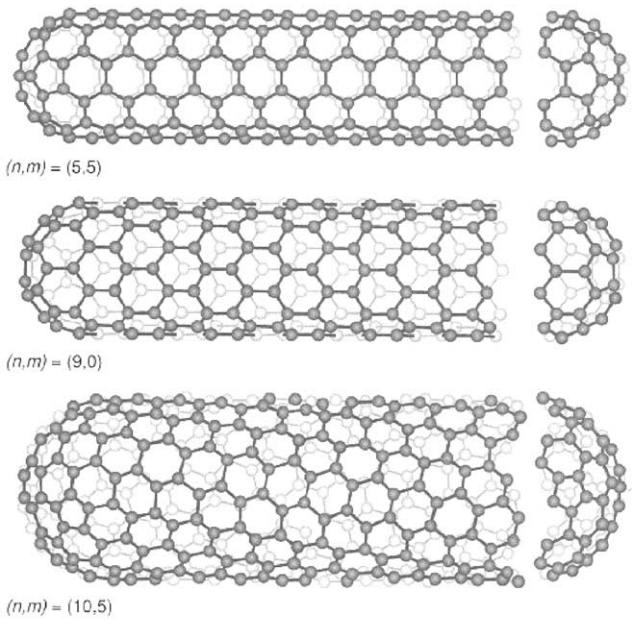

(a)

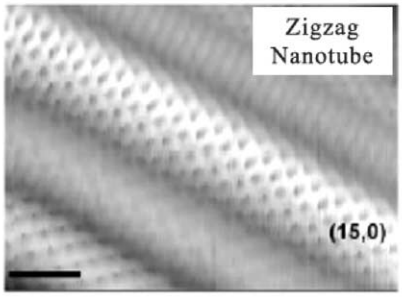

(b)

Fig. 9. (a) By rolling a graphene sheet into a cylinder and capping both ends to form nanotubes. Here is a schematic theoretical model for SWNT with different chirality: (top) armchair, (middle) zigzag and (bottom) chiral tubules [1]. (b) Atomic structure and spectroscopy of 'metallic' zigzag SWNTs captured by STM [29].

formula given in the table, the diameter of the nanotube could be determined once the chiral properties are measured.

3.2. Electronic and thermal properties

The electronic properties of nanotubes are sensitively depended on the nanotube's diameter and chirality [1,26]. These properties are uniquely characterised by the chiral vector as indicated in Eq. (1). The nanotubes possess metallic and semi-conducting properties by slightly changing of its size and chirality. Fig. 10 shows a two-dimensional graphene sheet along with the vector which specific the chiral nanotube and the metallic status of the nanotubes at specified chiral indices (n, m). Stroscio and Feenstra [31] have determined that armchair nanotubes $(n = m)$ have bands crossing the Fermi level and therefore possess metallic properties. However, for all other nanotubes with chiral indices of (n, m) and $(n, 0)$, two possible intrinsic properties exist. When $n - m = 3p$ (where p is an integer) such as (3, 0), (7, 1), (8, 5) and etc. the nanotubes are expected to be metallic. In the rest case $n - m \neq 3p$, the nanotubes are predicted to be semi-conducting materials with an energy gap of the order of $\sim$0.5 eV. This gap is highly dependent on the nanotube diameter and can be evaluated by

$$E_{\text{gap}} = \frac{2\gamma_0 a_{\text{C–C}}}{d} \tag{2}$$

where γ_0, $a_{\text{C–C}}$ and d denote the C–C tight-binding overlap energy (2.45 eV), the nearest neighbour C–C distance ($\sim$1.42 Å) and the diameter of the nanotube, respectively. In Fig. 11, a plot of the band gap energy (E_{gap}) versus the nanotube diameter (nm) ranging from 0.6 to 1.1 nm is given [32]. It is obviously seen that the band gap energy decreases with increasing the diameter of the nanotubes. The results were fitted with the chiralities of (10, 0), (11, 0), (14, −3) and (13, −1). Although many recent studies have been focused on the manufacturing process of identical nanotubes with the same diameter, the successful control of the chirality during the manufacturing process has not yet reported elsewhere.

Latest studies on the electronic properties of nanotubes have been focused on the tube–tube electrical transportability of the nanotubes at different contact positions [33–35]. The atomic structure in contact regions is crucial and the resistance of contracts varies sensitively with the nanotube geometry and chirality. For cross-junctions, low resistance was found when two nanotubes were in-registry and the contact region was commensurate. However, the contact resistance is highly susceptible to an externally applied force/pressure [35]. In Fig. 12(a) and (b), an experimental set up for measuring the conductance of a junction between two metallic SWNTs (5, 5) and the resistance measured by rotating the nanotubes to angles ranging from 0 to 180° are shown, respectively. In the figures, it is found that the conductance between two nanotubes is higher when two tubes are in-registry and the contact region is commensurate, where atoms from one tube are placed on top of another, i.e. for a junction (18, 0)–(10, 10), the $\theta =$ 30, 90 and 150° are in-registry while for a junction (10, 10)–(10, 10), the $\theta = 0$, 60, 120 and 180° are in-registry. For nanocomposite structures that are required to provide electrostatic discharge and as electromagnetic–radio frequency interference protection, the clarification of the resulting electrical properties, which are influenced by different nanotubes orientations inside the composites, are significant.

3.3. Mechanical properties

Many studies have addressed that nanotubes possess high

Table 1
Parameters of carbon nanotubes [30]

Symbol	Name	Formula	Value
a_{C-C}	Carbon–carbon distance		1.42 Å
a	Length of unit vector	$\sqrt{3}a_{C-C}$	2.46 Å
a_1, a_2	Unit vectors	$\left(\frac{\sqrt{3}}{2}, \frac{1}{2}\right)a, \left(\frac{\sqrt{3}}{2}, -\frac{1}{2}\right)a$	ln(x,y) coordinates
C_h	Chiral vector	$C_h = na_1 + ma_2 \equiv (n, m)$	n, m: integer
L	Circumference of nanotube	$L = \lvert C_h\rvert = a\sqrt{n^2 + m^2 + nm}$	$0 \le \lvert m\rvert \le n$
d	Diameter of nanotube	$d = \frac{L}{\pi} = \frac{\sqrt{n^2 + m^2 + nm}}{\pi}a$	
θ	Chiral angle	$\sin\theta = \frac{\sqrt{3}m}{2\sqrt{n^2 + m^2 + nm}}$	$0 \le \lvert\theta\rvert \le 30°$
		$\cos\theta = \frac{2n + m}{2\sqrt{n^2 + m^2 + nm}}$	
		$\tan\theta = \frac{\sqrt{3}m}{2n + m}$	

tensile modulus and strength as high as 1 TPa and 200 GPa, respectively. However, the scatterings of the measured results have been found in different literatures. An earlier report on the elastic modulus of defect-free nanotubes has been calculated in a straightforward way by using the properties of graphite was approximately as 1060 GPa [7,36]. Ruoff and Lorents [37] have estimated that the tensile strength of nanotubes with a wall thickness and diameter of 0.34 and 1 nm, respectively, was about 20 GPa and its natural frequency of the cantilevered SWNT with a length of 1 μm was about 12 MHz. Yu et al. [38] has demonstrated the use of atomic force microscopy (AFM) to measure the mechanical properties of MWNTs in the SEM. They measured that the tensile strength and modulus of the nanotubes were ranging from 11 to 63 GPa, and 270 to 950 GPa, respectively. It was found that an outer layer of the

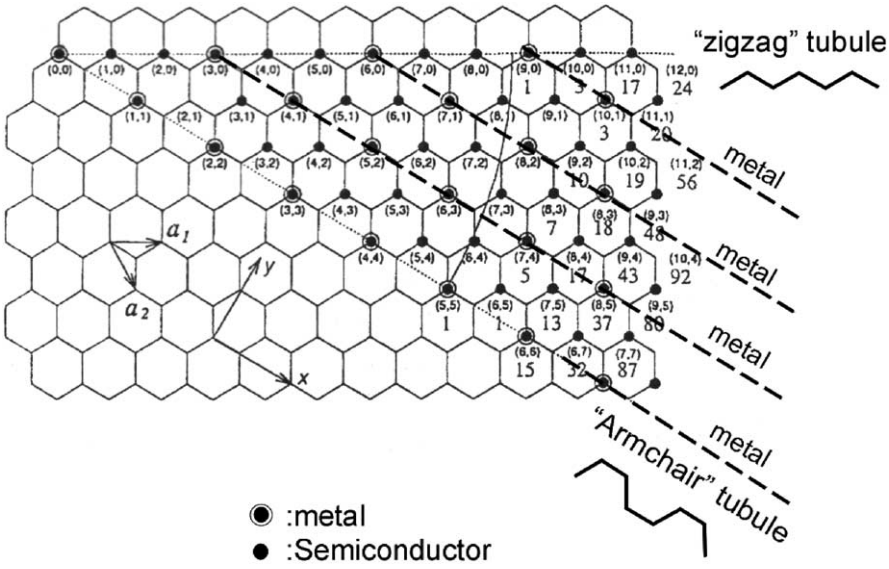

Fig. 10. The two-dimensional graphene sheet with given chiralities (n, m).

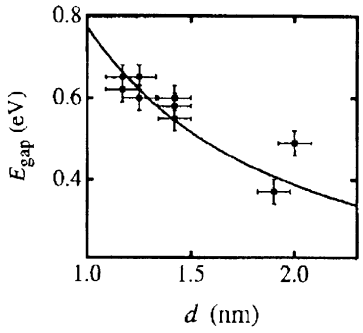

Fig. 11. Energy gap E_{gap} versus diameter d of the nanotubes with a conducting chirality. The solid line denotes the theoretical prediction of Eq. (2) with a γ_0 of 2.7 eV [28].

nanotubes was initially failed during the test. The maximum strain could be achieved to about 12% at failure. The SEM images of a nanotube linked between two opposing AFM tips before tensile loading are shown in Fig. 13. Wong et al. [39] have studied the bending stiffness of cantilevered MWNTs via the lateral movement of an AFM tip. They found that the nanotubes were able to sustain a large elastic deformation without breakage, enabling them to be designed for applications that are required storing or absorbing considerable energy. Vigolo et al. [40] found that the SWNT fibres could be knotted tightly without breakage and exhibited a plastic behaviour, which is difference with conventional carbon fibres at room temperature before they break. The tensile modulus measured during the experiment was about 15 GPa as shown in Fig. 14.

Tersoff and Ruoff [41] found that nanotubes with a diameter less than 1 nm behaved high rigidity. Any nanotubes with a diameter beyond 2.5 nm appeared radial deformation 'flatten' due to the van der Waals attraction. The extent of radial deformation increases as the diameter is increased. In Fig. 15, it is clearly shown that the distortions arising when two single-walled armchair nanotubes cross each other and non-circular cross-section in an overlap region is resulted. It was computed that the force acting on a low nanotube was about 5 nN [42]. The bottom of the figure also depicts the radial deformation of the SWNT due to van der Waals interaction with a graphite surface. It is found that the attraction forces tend to flatten the bottom of the tubes so as to increase the contact area,

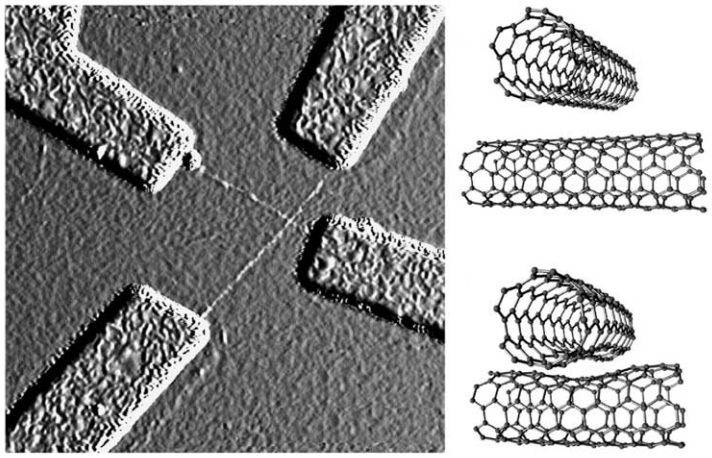

(a)

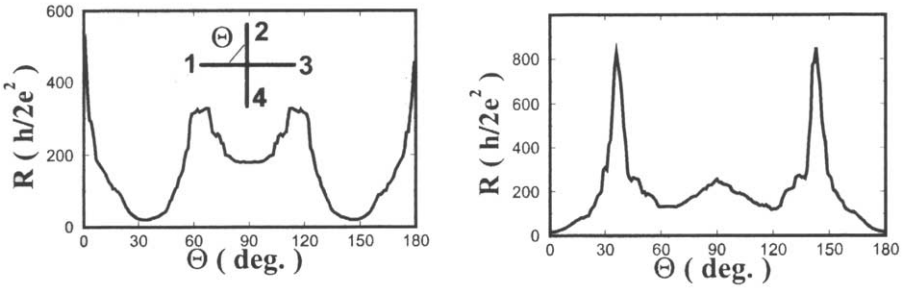

(b)

Fig. 12. (a) Left—tapping-mode AFM image of a crossed single-walled device. The nanotubes are located at the middle of the diagram and spanned between the Cr/Au electrodes [34]; right—the structures used to calculate the conductance of a junction between two armchair nanotubes. (b) Resistance of four-terminal nanotube junction as a function of tube rotation: (Left) a (18, 0)–(10, 10) junction and (right) a (10, 10)–(10, 10) junction [35].

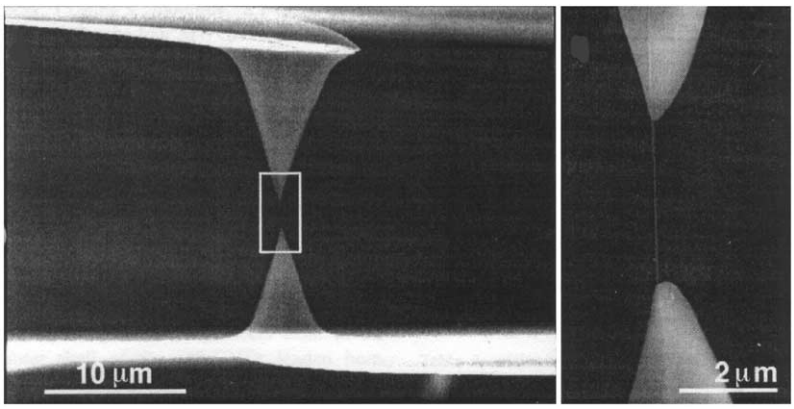

Fig. 13. The SEM images of a nanotube linked between two opposing AFM tips before tensile loading [37].

which is increased with increasing the radius of the nanotubes.

Robertson et al. [43] has computed the strain energy of nanotubes by using a continuum elastic model [44]. They concluded that the nanotubes behave softly in small radius and chiral angle θ, i.e. the two zigzag and armchair nanotubes yield the lower and upper limits of the stiffness along the tube's axis, respectively, for a given radius. Nardelli et al. [45] have used a molecular dynamics simulation to study the mechanical performance of nanotubes under uniaxial tensile load and different temperature conditions. They reported that armchair nanotubes could release its excess strain when undergoing uniaxial tensile stress via the spontaneous formation of a Stone–Wales defect, which is formed by a nucleation of a dislocation loop in the hexagonal network of the graphite sheet through the reallocation of C–C bond producing a two pentagonal and two heptagons structure as indicated in Fig. 16. The atoms that take part in the Stone–Wales transformation are highlighted in a small circular spot at the centre of the atoms. Nardelli et al. [45] have also calculated that all nanotubes are brittle in a high strain and low temperature condition, while at a low strain and high temperature situation armchair nanotubes behave

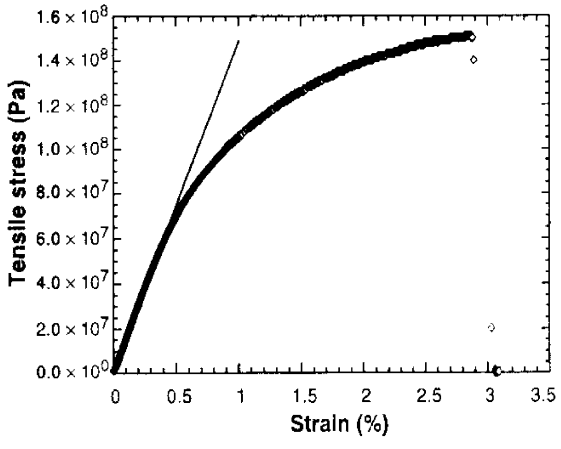

Fig. 14. Stress versus strain of the SWNTs fibre [40].

completely ductile. For zigzag nanotubes with $n < 14$, the material properties behave partly ductile while larger nanotube are completely brittle. In Fig. 17(a), the ductile–brittle domain map for carbon nanotubes with a diameter up to 13 nm is shown. In reality, for SWNTs under uniaxial tensile loading, both ductile and brittle properties exist simultaneously once the first Stone–Wales defect occurred. This is due to the breakage of bond under strain and the occurrence of dislocation in the nanotubes [46]. Fig. 17(b) demonstrates the process of defect of the nanotube subjected to a high stress and temperature condition with an initial Stone–Wales defect at the middle of the nanotube. Further details in the relation to the mechanism of strain release due to lattice distortion and dislocation of nanotubes could be found in Refs. [47,48].

Rochefort et al. [49] have studied computationally the bending and twisting properties of nanotubes. They found that the increase of the electrical resistance of the nanotubes with increasing the bending angle, particularly at the angle higher than 45° when the strain is strong enough to lead to kinks in an nanotube structure. For an armchair nanotube, the band gap energy increases linearly with increasing the twisting angle up to a critical limit. Twisting above this angle may cause the collapse of the nanotube structure and the formation of a flattened helix. In Fig. 18, the molecular mechanic computational model and the computed band gap energy using extended Huckel theory versus twisting angle are shown. Poncharal et al. [50] have observed that the bending modulus of nanotubes decreases rapidly with increasing the diameter of the nanotube. This drop of elastic modulus might be due to the formation of wavelike distortions in the nanotube as shown in Fig. 19. Falvo et al. [51] have concluded that nanotubes could be sustained repeated bending as high as a local strain up to 16% without failure. Yakobson et al. [52] and Ru [53,54] have used a continuum shell and multi-shell elastic models, respectively, to study the bucking behaviour of nanotubes under uniaxial compressive loads. They concluded that the nanotubes are remarkably resilient, it could be sustained a large strain with no sign of brittleness, plasticity or atomic rearrangement.

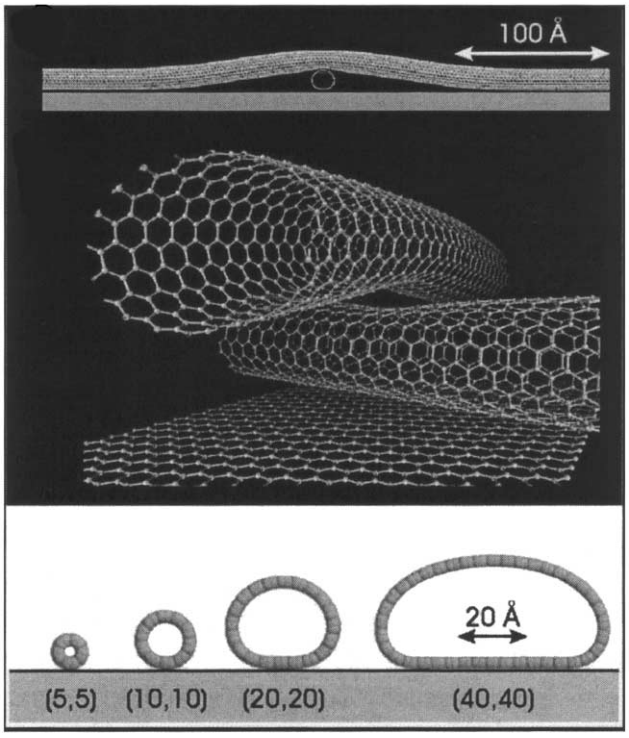

Fig. 15. Molecular mechanics calculations on axial and radial deformations of SWNTs for (top) two crossed armchair tubes and (bottom) SWNTs on graphite [42].

4. Nanotubes composites

Since the discovery of nanotubes, extensive research in carbon, fullerence, nanosensor, nanoindentator and nanomachine has blossomed in many different directions, and has attracted a great deal of attention to advanced composite society. It is well understood that carbon fibres or nanotubes could not be utilised alone without any supporting medium, such as matrix to form structural components. Whereas, the investigation on the interfacial bonding properties between the nanotube and matrix system is of a great interest, which ensures a good stress transfer between the nanotube and matrix of nanocomposite structures in the development of nanotube composites.

In 1998, Lourie et al. [55] has started investigating the buckling and collapse of carbon nanotubes/epoxy composite structures. They found that the shrinkage of an epoxy matrix after curing could generate a substantial high compressive stress to embedded nanotubes. Therefore, the different levels of buckling of the nanotubes happened. Bent and loop shapes of the buckled nanotubes were observed under the TEM. The outer surface of the nanotubes, in turn sustained a high flexural strength due to the formation of a sharp turn. These phenomena, however, do not be considered in macro-scale composite systems because of the stiffness of fibres is relatively strong enough to overcome the shrinkage stress induced by the matrix. Hadjiev et al. [56] have found the similar observation that the residual stress of less than 70 MPa existed on embedded nanotubes due to epoxy shrinkage in the curing process. In Fig. 20, the buckled MWNTs subjected to compressive stress due to the shrinkage of the matrix are shown by the TEM.

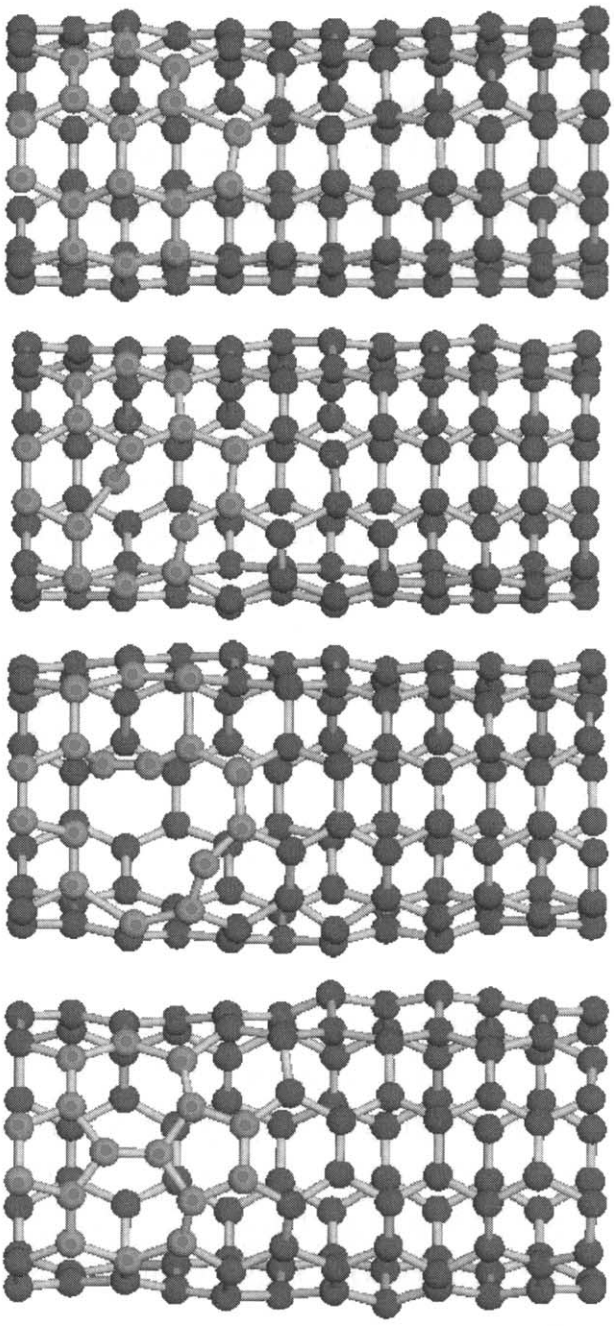

Fig. 16. Kinetic mechanism of the Stone–Wales defect formation from quantum mechanical molecular dynamics simulation for an armchair nanotube (5, 5) at 1800 K [47].

Recently literatures [57–59] reported that the Raman spectroscopy could be used to measure the strain of nanotube composites by measuring a peak signal shift of the Raman spectra to identify the strain conditions of the

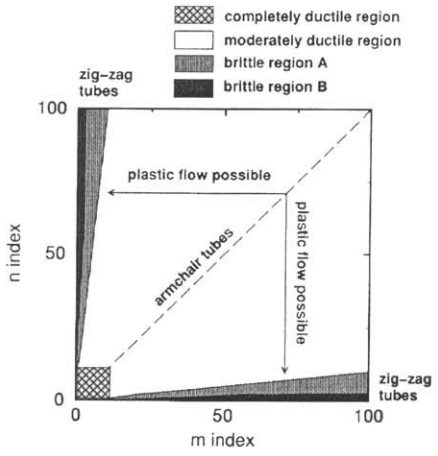

(a)

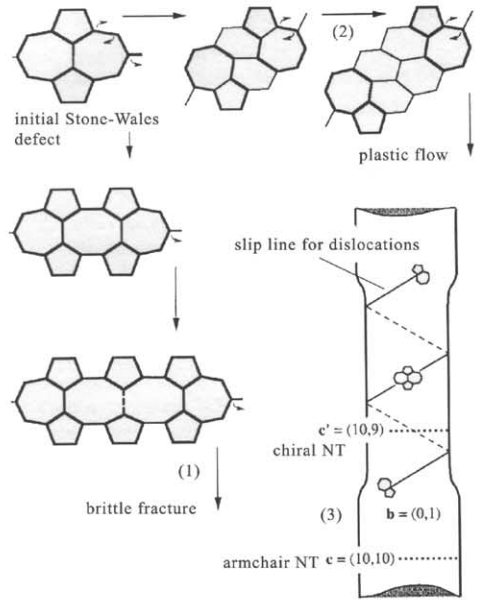

(b)

Fig. 17. (a) Ductile–brittle domain map for carbon nanotubes with diameters up to 13 nm. Different shaded areas correspond to different possible materials behaviours [45]. (b) The process of defect of an armchair nanotube with an initial Stone–Wales defect. (1) A brittle crack; (2) a couple of dislocation gliding away from each other; (3) the change of the nanotube chirality and a stepwise change of diameter causes the corresponding variation of electrical properties. Formation of a next Stone–Wales defect continues the necking process, unless the dislocations pileup at insufficient temperature [46].

composites. Schadler et al. [57] and Wood et al. [58] have studied the use of the Raman spectroscopy technique to measure the strain of the nanotube composites. They found that the compressive modulus of the nanotube is higher than the tensile modulus. The Raman peak shift could indicate the strain condition of the composites. Cooper et al. [59] have demonstrated the Raman spectra of a nanotube composite beam subjected to four-point bending. The spectra shifted downward with an increase of the tensile strain on the beam surface as indicated in Fig. 21. A curve plotted (inside a small box) in the diagram shows the Raman peak shift of the nanotube composites with the surface strain is increased.

Since the load transfer properties are the main issues that ensure the composite system is functioned properly, the investigation on the interfacial shear stress between embedded nanotubes and matrix is significant. There are three main load transfer mechanisms that control the full operation of the stress transfer, they include micro-mechanical interlock, chemical bonding (interaction) and a weak van der Waals attractive force. The first one is typically uninfluenced to the nanocomposite system since the surface of the nanotubes appears atomically smooth. Wagner et al. [60] have reported that the interfacial bonding stress between the nanotubes and polymer could be reached as high as 500 MPa. Lordi and Yao [3] have found that the sliding friction between nanotube surface and polymer substrate was much greater than that between two graphene sheets. Jin et al. [61] and Bower et al. [62] have focused on the bonding behaviour of nanotubes to polymeric materials. They found that the nanotubes have physically contacted well with the matrix (polyhydroxyaminoether). However, no fractures of the nanotubes were observed at the fracture surface of the nanotube composite. This indicated that the load transfer from the polymer to the nanotube was not sufficiently large enough to break the nanotubes. In Fig. 22(a), the fracture surface of a nanotubes composite is shown. Another amazing result was found: the nanotube could restore to its original un-buckled shape when the matrix was heated up, i.e. the compressive stress due to the shrinkage of the cured matrix could be released. Fig. 22(b) is clearly showed the difference of the embedded nanotube before and after heating up the nanotube composite.

Qian et al. [63] have reported that by adding 1% of nanotubes into polystyrene matrices resulted in increases of overall tensile modulus and strength by approximately 42 and 25%, respectively. They also observed via TEM micrographs that the nanotubes were able to bridge the crack surface of the composite once a crack was initiated. The crack was nucleated at low nanotube density area and propagated towards a region with relatively low nanotube density regions. Pull out of the nanotubes was observed when the crack opening displacement reached ≈800 nm.

Sandler et al. [64] have studied the electrical properties of composites with randomly dispersing nanotubes, which acted, as conductive fillers into an epoxy matrix in order to avoid electrostatic charge existed in composite structures. They found that the use of small fraction of nanotubes in place of carbon black could provide sufficient matrix conductivity (up to 6×10^{-3} S m^{-1}) for anti-static applications. Andrews et al. [65] have used bundles of nanotubes and petroleum-derived pitch matrix to form composites.

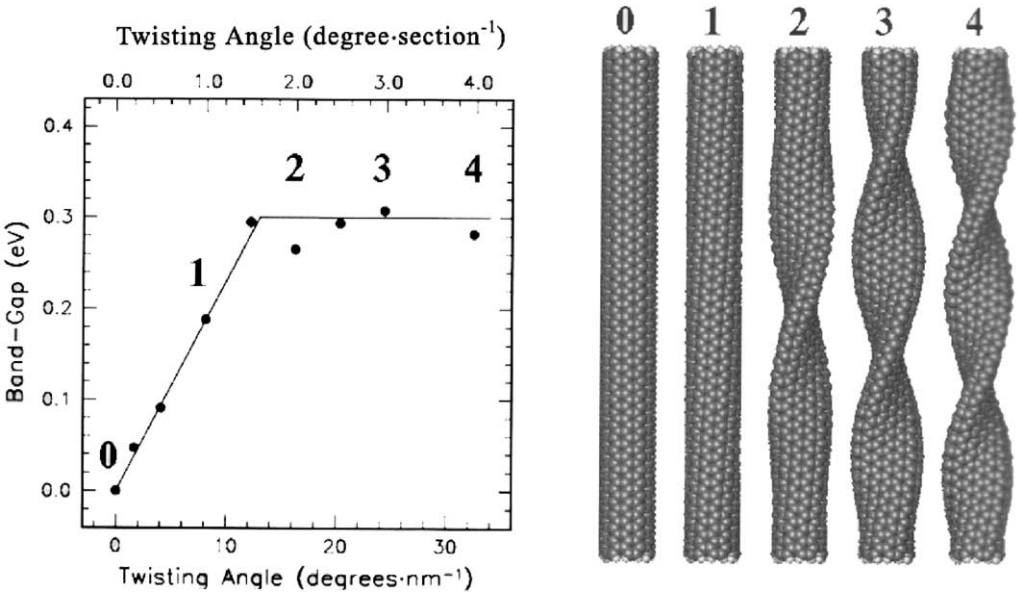

Fig. 18. Molecular mechanic computational model and the computed band gap energy using extended Huckel theory versus twisting angle [49].

They found that the overall tensile strength increases with increasing the fraction of nanotubes inside the composites. However, a good alignment for all nanotubes could not be guaranteed.

5. Other applications

Due to many unique properties of the nanotubes, the potentiality of its applications in real-life practice has been recently emerged. Dzegilenko et al. [66] have computed that nanotubes could be used as nanoetcher and nanoindentor to extract silicon atoms from the silicon surface robustly without additionally involving an externally applied voltage via molecular dynamic simulation.

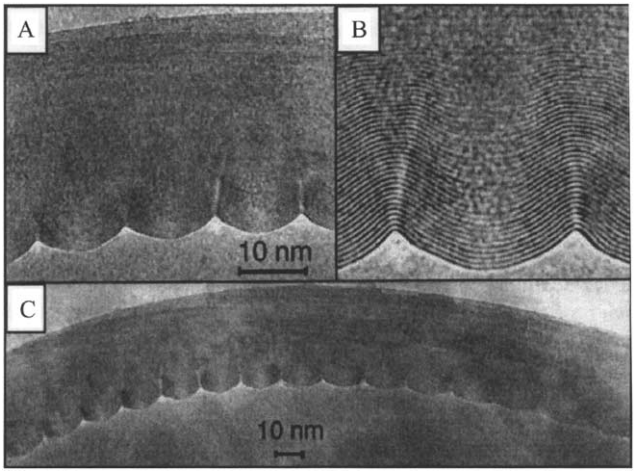

Fig. 19. TEM images of a bent nanotube with a radius of curvature ~40 nm; (A and B) high magnified view of (C). The amplitude of the ripples increases towards the outer layer of the nanotube [50].

Avouris et al. [42] have demonstrated the use of a nanotube bundle as an electrode in nanoscale tip-induced anodisation. In Fig. 23, a bundle of MWNTs was used as a tip to locally oxidise a silicon plate surface and generate the oxide pattern of 'C-tube'. Cumings and Zettl [67] have investigated the frictional properties between MWNTs. The friction between the individual nanotube is bound by a weak van der Waals force. The results revealed that the MWNTs hold a great promise for nanomechanical or nanoelectromechanical systems applications. A four-shell core nanotube could be eased to withdraw without any damages (Fig. 24). This leads to the design of low friction and low wear bearings, springs and electromechanical switches in a nanoscale. Many researches [68–70] have been still carrying out on the electrical transportability, mechanical performance and control of manufacturing process in terms of quality and geometry of nanotubes and nanotube composites in order to clarify most practical problems before applying these structures in real-life applications.

6. Concluding remarks

In the last decade, extensive research in nanotubes has been found increasingly. The majorities were paid attentions on its electrical, mechanical and functional properties. However, there are no universal conclusions have been made on each of those works because of the material and geometrical properties of nanotube(s) used in the works were inconsistent. In the past few years, works related to nanotube composites including the investigation on the interfacial bonding properties and morphological observations through microscopy have appeared in a few literatures. In depth study on the stress transfer mechanism of the

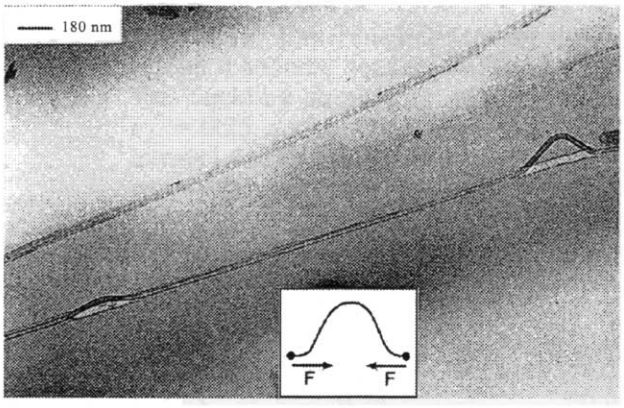

(a)

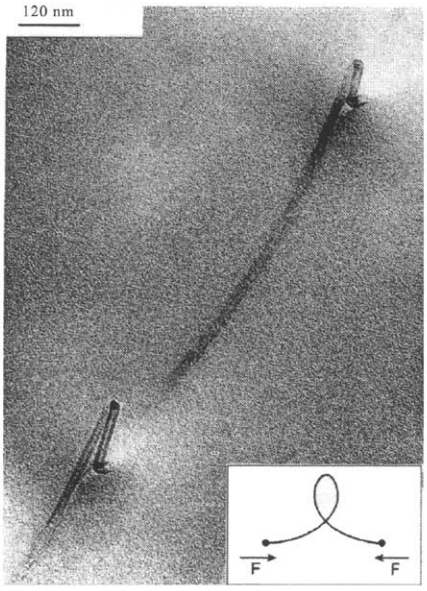

(b)

Fig. 20. TEM images of embedded MWNTs. (a) The bent and (b) loop forms of nanotubes under compression (shrinkage of the matrix) [55].

nanotube composites with different chemical and geometrical properties, matrix environments and loading conditions are essential although many superficial works have previously addressed that the nanotubes have a good chemical bonding with typical polymeric materials. The reliability, thermal-mechanical properties and atomic relocation due to chemical interaction between carbon atoms and matrix are important issues that should be studied. The potential applications of using the nanotubes in real-life applications are huge ranging from genetic probe, mechanical memory and nanoweezers, nanosensitive sensor, hydrogen and ion storage, nanoetcher, nanoindentor and nanofiller for nanocomposite structures [23]. It is dependent on how to utilise fully the extraordinary properties of

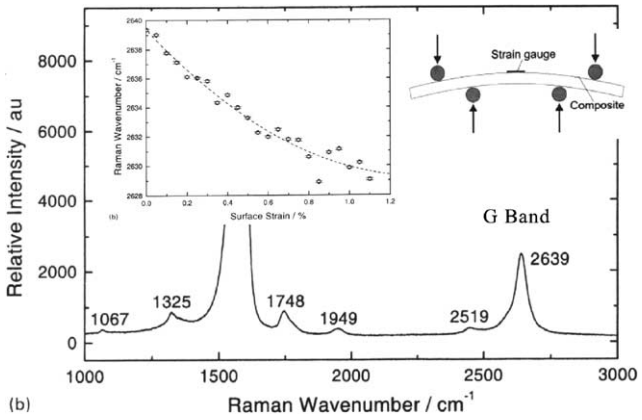

Fig. 21. Raman spectra of the SWNT composite beam subjected to four-point bending. The peak of the G band shifts downward with increasing the tensile strain on the composite surface [59].

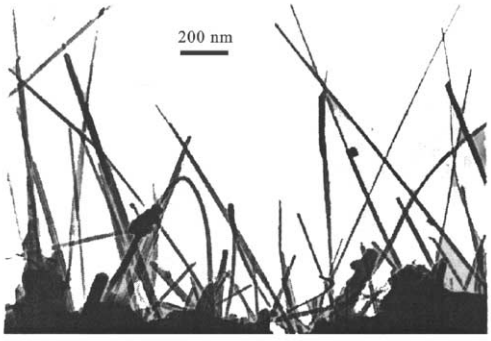

(a)

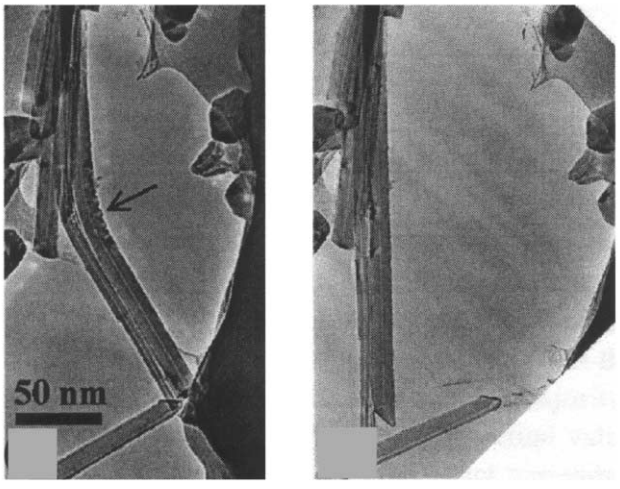

(b)

Fig. 22. (a) Fracture surface of a nanotube composite; (b) Two TEM images show the original bent nanotube (left) at room temperature and (right) after heating up [62].

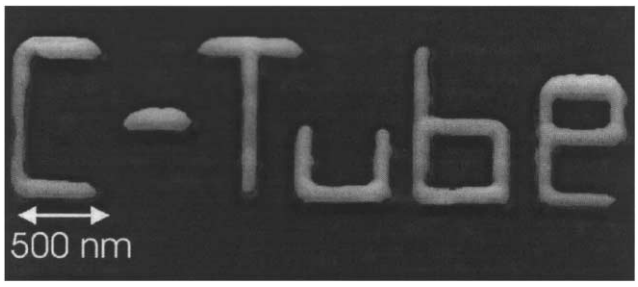

Fig. 23. The use of conducting carbon nanotube AFM tips as nanofabrication tools [42].

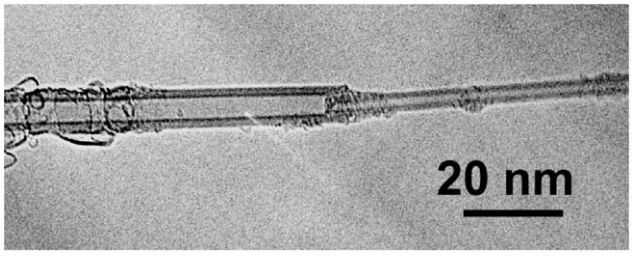

Fig. 24. A TEM image of a telescoped nanotube. The four-shell core section of the nanotube has been extracted [67].

the nanotubes in different applications. This paper reports recent development related to nanotubes and nanotube composites. After grouping up all concluding remarks from literatures, it has been found that there are still a numerous problems that should be solved before putting these advanced materials into a real life. For an instance, only randomly oriented nanotube composite structures could be made up-to-date. How to control the alignment of the nanotubes during manufacturing process is one of the big impacts for the design of nanotube composites.

In the future, there is no doubt that the nanotechnology will be one of the emerging technologies that will play a significant role in developing future space vehicles. The development of a new manufacturing process of nanotubes with high purity, geometrical identity and productivity, and low cost is an important factor in bringing the nanotubes to be more acceptable to the society.

Acknowledgements

This work was supported by The Hong Kong Polytechnic University Grant (G-YW60) and the University of New Orleans (Graduate Enhancement Fund).

References

[1] Dresselhaus MS, Dresselhaus G, Eklund PC, editors. Science of fullerences and carbon nanotubes. London: Academic Press, 1996.
[2] Iijima S. Helical microtubles of graphitic carbon. Nature (London) 1991;354:56–8.
[3] Lordi V, Yao N. Molecular mechanics of binding in carbon-nanotube-polymer composites. J Mater Res 2000;15:2770–9.
[4] Files BS. Application of carbon nanotubes for human space exploration. Proceedings of Nanospace'98.
[5] Files BS. Processing of carbon nanotubes for revolutionary space applications. AIAA-2000-5345; 2000.
[6] Harris PJF, editor. Carbon nanotubes and related structures, new materials for the twenty-first century. UK: Cambridge University Press, 2000.
[7] Lu JP. Elastic properties of single and multilayered nanotubes. J Phys Chem Solids 1997;58:1649–52.
[8] Li F, Cheng BS, Su G, Dresselhaus MS. Tensile strength of single-walled carbon nanotubes directly measured from their macroscopic ropes. Appl Phys Lett 2000;77:3161–3.
[9] Journet C, Bernier P. Production of carbon tubes. Appl Phys, A 1998;67:1–9.
[10] Journet C, Maser WK, Bernier P, Loiseau A, Lamy de la Chapelle M, Lefrant A, Deniard P, Lee R, Fischer JE. Large-scale production of single-walled carbon nanotubes by the electric-arc technique. Nature 1997;388:756–8.
[11] Yakobson BI, Smalley RE. Fullerence nanotubes: $C_{1,000,000}$ and beyond. Am Scient 1997;July–August.
[12] Rinzler AG, Liu J, Dai H, Nikolaev P, Huffman CB, Todriguez-Macias FJ, Boul PJ, Lu AH, Heymann D, Colbert DT, Lee RS, Fischer JE, Rao AM, Eklund PC, Smalley RE. Large-scale purification of single-wall carbon nanotubes: process, product, and characterisation. Appl Phys, A 1998;67:29–37.
[13] Endo M, Takeuchi K, Kobori K, Takahashi K, Kroto HW, Sarkar A. Pyrolytic carbon nanotubes from vapor-grown carbon fibres. Carbon 1995;33:873–81.
[14] Nikolaev P, Bronikowski MJ, Bradley RK, Fohmund F, Colbert DT, Smith KA, Smalley RE. Gas-phase catalytic growth of single-walled carbon nanotubes from carbon monoxide. Chem Phys Lett 1999;313:91–7.
[15] Schlittler RR, Seo JW, Gimzewski JK, Durkan C, Saifullah MSM, Welland ME. Single crystals of single-walled carbon nanotubes formed by self-assembly. Science 2001;292:1136–9.
[16] Qin LC, Zhou D, Krauss AR, Gruen DM. Growing carbon nanotubes by microwave plasma-enhanced chemical vapor deposition. Appl Phys Lett 1998;72:3399–517.
[17] Qin LC, Iijima S. Structure and formation of raft-like bundles of single-walled helical carbon nanotubes produced by laser evaporation. Chem Phys Lett 1997;269:65–71.
[18] Terrones M, Grobert N, Olivares J, Zhang JP, Terrones H, Kordatos K, Hsu WK, Hare JP, Townsend PD, Prassides K, Cheetham AK, Kroto HW, Walton DRM. Controlled production of aligned-nanotube bundles. Nature 1997;388:52–5.
[19] Thostenson ET, Ren ZF, Chou TW. Advances in the science and technology of carbon nanotubes and their composites: a review. Compos Sci Technol 2001;61:1899–912.
[20] Fan S, Chapline MG, Franklin NR, Tombler TW, Cassell AM, Dai H. Self-oriented regular arrays of carbon nanotubes and their field emission properties. Science 1999;283:512–4.
[21] Bower C, Zhu W, Jin SH, Zhou O. Plasma-induced alignment of carbon nanotubes. Appl Phys Lett 2000;77:830–2.
[22] Saito Y, Nishikubo K, Kawabata K, Matsumoto T. Carbon nanocapsules and single-layed nanotubes produced with platinum-group metals by arc discharge. J Appl Phys 1996;80:3062–7.
[23] Collins PG, Avouris P. Nanotubes for electronics, vol. 283. Scientific American Inc, 2000 p. 62–9.
[24] Feynman RP. There's plenty of room at the bottom. J Microelectromech Syst 1992;1:60–6.
[25] Port O. It's nano world. Buss Week 2000;November 27.
[26] Mintmire JW, White CT. Electronic and structural properties of carbon nanotubes. Carbon 1995;33:893–902.
[27] Dresselhaus MS, Dresselhaus G, Saito R. Carbon fibers based C_{60} and their symmetry. Phys Rev B 1992;45:6234–42.

[28] Wildoer JWG, Venema LC, Rinzler AG, Smalley R, Dekker C. Electronic structure of atomically resolved carbon nanotubes. Nature 1998;391:59–62.
[29] Ouyang M, Huang JL, Cheung CL, Lieber CM. Energy gaps in metallic single-walled carbon nanotubes. Science 2001;292:702–5.
[30] Dresselhaus MS, Dresselhaus G, Saito R. Physics of carbon nanotubes. Carbon 1995;33:883–91.
[31] Stroscio JA, Feenstra RM. In: Stroscio JA, Kaiser WJ, editors. Scanning tunnelling microscopy. New York: Academic Press. 1993 p. 95–141.
[32] Odom TW, Huang JL, Kim P, Lieber CM. Atomic structure and electronic properties of single-walled carbon nanotubes. Nature 1998;391:62–4.
[33] Paulson S, Helser A, Nardelli MB, Taylor II RM, Falvo M, Superfine R, Washburn S. Tunable resistance of a carbon nanotube–graphite interface. Science 2000;290:1742–4.
[34] Fuhrer MS, Nygard J, Shih L, Forero M, Yoon YG, Mazzoni MSC, Choi HJ, Ihm J, Louie SG, Zettl A, Mceuen PL. Crossed nanotube junctions. Science 2000;288:494–7.
[35] Buldum A, Lu JP. Contact resistance between carbon nanotubes. Phys Rev B 2001;6316:1403–6.
[36] Kelly BT, editor. Physics of graphite. London: Applied Science, 1981.
[37] Ruoff RS, Lorents DC. Mechanical and thermal properties of carbon nanotubes. Carbon 1995;33:925–30.
[38] Yu MF, Lourie O, Dyer M, Moloni K, Kelly TF, Ruoff RS. Strength and breaking mechanism of multi-walled carbon nanotubes under tensile load. Science 2000;287:637–9.
[39] Wong EC, Sheehan PE, Lieber CM. Nanobeam mechanics: elasticity, strength, and toughness of nanorods and nanotubes. Science 1997;277:1971–5.
[40] Vigolo B, Penicaud A, Coulon C, Sauder C, Pailler R, Journet C, Bernier P, Poulin. Macroscopic fibers and ribbons of oriented carbon nanotubes. Science 2000;290:1331–4.
[41] Tersoff J, Ruoff RS. Structural properties of a carbon-nanotube crystal. Phys Rev Lett 1994;73:676–9.
[42] Avouris P, Hertel T, Martel R, Schmidt T, Shea HR, Walkup RE. Carbon nanotubes: nanomechanics, manipulation, and electronic devices. Appl Surf Sci 1999;141:201–9.
[43] Robertson DH, Brenner DW, Mintmire JW. Energetics of nanoscale graphitic tubules. Phys Rev B 1992;45:12592–5.
[44] Tibbetts GG. Why are carbon filaments tubular? J Cryst Growth 1984;66:632–8.
[45] Nardelli MB, Yakobson BI, Bernholc J. Brittle and ductile behaviour in carbon nanotubes. Phys Rev Lett 1998;81:4656–9.
[46] Yakobson BI. Mechanical relaxation and intermolecular plasticity in carbon nanotubes. Appl Phys Lett 1998;72:918–20.
[47] Nardelli MB, Yakobson BI, Bernholc J. Mechanism of strain release in carbon nanotubes. Phys Rev B 1998;57:4277–80.
[48] Dresselhaus MS, Dresselhaus G, Avouris Ph, editors. Carbon nanotubes: synthesis, structure, properties, and applications. Berlin: Springer, 2001.
[49] Rochefort A, Avouris P, Lesage F, Salahub DR. Electrical and mechanical properties of distorted carbon nanotubes. Phys Rev B 1999;60:13824–30.
[50] Poncharal P, Wang ZL, Ugarte D, Heer WAd. Electrostatic deflections and electromechanical resonances of carbon nanotubes. Science 1999;283:1513–6.
[51] Falvo MR, Clary GJ, Taylor RM, Chi V, Brook FP, Washburn S, Superfine R. Bending and bucking of carbon nanotubes under large strain. Nature 1997;389:582–4.
[52] Yakobson BI, Brabec CJ, Bernholc J. Nanomechanics of carbon tubes: instabilities beyond linear response. Phys Rev Lett 1996;76:2511–4.
[53] Ru CQ. Effective bending stiffness of carbon nanotubes. Phys Rev B 2000;62:9973–6.
[54] Ru CQ. Degraded axial buckling strain of multiwalled carbon nanotubes due to interlayer slip. J Appl Phys 2001;89:3426–33.
[55] Lourie O, Cox DM, Wagner HD. Buckling and collapse of embedded carbon nanotubes. Phys Rev Lett 1998;81:1638–41.
[56] Hadjiev VG, Live MN, Arepalli S, Nikolaev P, Files BS. Raman scattering test of single-wall carbon nanotube composites. Appl Phys Lett 2001;78:3193–5.
[57] Schadler LS, Giannaris SC, Ajayan PM. Load transfer in carbon nanotube epoxy composites. Appl Phys Lett 1998;73:3842–4.
[58] Wood JR, Zhao Q, Wagner HD. Orientation of carbon nanotubes in polymers and its detection by Raman spectroscopy. Composites: Part A 2001;32:391–9.
[59] Cooper CA, Young RJ, Halsall M. Investigation into the deformation of carbon nanotubes and their composites through the use of Raman spectroscopy. Composites: Part A 2001;32:401–11.
[60] Wagner HD, Lourie O, Feldman Y, Tenne R. Stress-induced fragmentation of multiwall carbon nanotubes in a polymer matrix. Appl Phys Lett 1998;72:188–90.
[61] Jin L, Bower C, Zhou O. Alignment of carbon nanotubes in a polymer matrix by mechanical stretching. Appl Phys Lett 1998;73:1197–9.
[62] Bower C, Rosen R, Jin L, Han J, Zhou O. Deformation of carbon nanotubes in nanotube-polymer composites. Appl Phys Lett 1999;74:3317–9.
[63] Qian D, Dickey EC, Abdrews R, Rantell T. Load transfer and deformation mechanisms in carbon nanotube-polystyrene composites. Appl Phys Lett 2000;76:2868–70.
[64] Sandler J, Shaffer MSP, Prasse T, Bauhofer W, Schulte K, Windle AH. Development of a dispersion process for carbon nanotubes in an epoxy matrix and the resulting electrical properties. Polymer 1999;40:5967–71.
[65] Andrews R, Jacques D, Rao AM, Rantell T, Derbyshire F, Chen Y, Chen J, Haddon RC. Nanotube composite carbon fibers. Appl Phys Lett 1999;75:1329–31.
[66] Dzegilenko F, Srivastava D, Saini S. Nanoscale etching and indentation of a silicon (001) surface with carbon nanotube tips. Nanotechnology 1999;10:253–7.
[67] Cumings J, Zettl A. Low friction nanoscale linear bearing realized from multiwall carbon nanotubes. Science 2000;289:602–4.
[68] Ting JM, Chang CC. Multi-junction carbon nanotube network. Appl Phys Lett 2002;80:324–5.
[69] Park JW, Kim J, Lee JO, Kang KC, Kim JJ, Yoo KH. Effects of artificial defects on the electrical transport of single-walled carbon nanotubes. Appl Phys Lett 2002;80:133–5.
[70] Pablo PJ, Gomez-Navarro C, Colchero J, Serena PA, Gomez-Herrero J, Baro AM. Nonlinear resistance versus length in single-walled carbon nanotubes. Phys Rev Lett, in press.